Pseudo-Static Test of Mixed Connections Between Steel Columns and Concrete Columns in Pudong (Shanghai) International Airport Terminal 2

J. Zhang[1]; X. L. Lu[2]; and W. C. Luo[3]

[1] *Ph.D Candidate, State Key Laboratory for Disaster Reduction in Civil Engineering, Tongji University, Shanghai, China*
[2] *Professor, State Key Laboratory for Disaster Reduction in Civil Engineering, Tongji University, Shanghai, China*
[3] *Structural Engineer, Shanghai Institute of Mechanical & Electrical Engineering Co., Ltd, Shanghai, China*
Email: jiezhang000@gmail.com, lxlst@mail.tongji.edu.cn, lwc99999@hotmail.com

ABSTRACT :

Mixed columns, consisting of a steel upper portion and a concrete lower portion, were used in the construction of Pudong International Airport Terminal 2. Two types of joints were designed for connections between the steel roof and concrete columns. The first is a cast steel bearing, connecting inclined steel branches and the supporting concrete member; the second is a direct embedment of the inclined steel branch into the concrete column.

In order to evaluate the mechanical behavior and reliability of these mixed connections, pseudo-static tests were carried out at Tongji University. Results and conclusions from this investigation include: 1) cracking and spalling were observed at the top of the concrete columns due to the moment applied by the upper steel columns and abrupt variation of column stiffness near the joint. Additional stirrups or an exterior steel tube are suggested to enhance shear capacity and improve confinement of the outer concrete. 2) Damage occurring at the bottom of the steel column could be attributed to the modulus of elasticity and yield strength of the steel both being decreased about 10% in the Heat Affected Zone (HAZ) as well as higher than expected strength of the cast steel. The damage observed near the butt weld showed great similarity to that of steel structures in the Kobe earthquake 1995. 3) A potentially critically damaged section was identified in the cast steel bearing based on the numerical and experimental results, however it remained undamaged in the test. Since the strength of the cast material is more inconsistent than hot rolled steel; a larger variance will be used to for the design strength. Therefore, the actual capacity of the cast steel bearing is more likely to be under-estimated and the performance of the cast steel may not be as expected in the original design. 4) Additionally, based on the analyses of loading transfer mechanism and calculation of elastic rotational stiffness with respect to cast steel bearings, mechanical behavior and deformation capacity of the bearings were investigated. A component of displacement at the top of steel columns was examined as well.

KEYWORDS: mixed columns, mixed connections, cast steel bearing, pseudo-static test

1. INTRODUCTION

Phase II of Pudong International Airport has a total floor area of 400,000 square meters and constitutes Terminal 2, a boarding hall, and mass transit stations that link terminals together. Terminal 2 was designed with steel roof, concrete frame, and mixed column connecting members. The mixed columns are connected with beam strings to resist lateral loads applied to the roof (See Fig. 1).

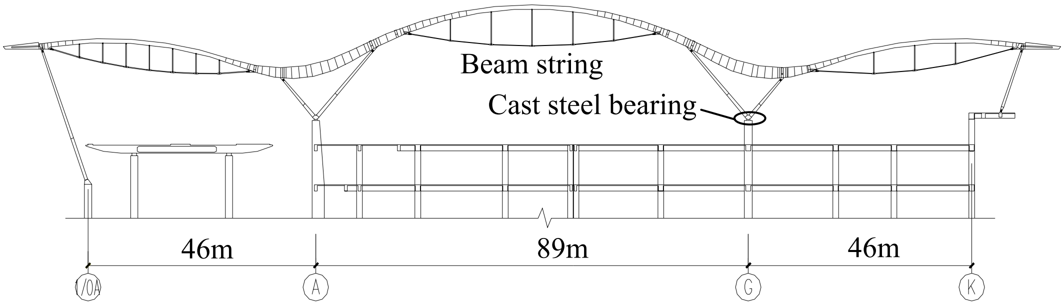

Figure 1 Elevation view of terminal building

There are two types of mixed columns in the structure. V-shaped steel columns and supporting concrete columns are linked with cast steel bearings to form the mixed columns along gridlines A and G, while inclined steel columns are embedded directly into concrete columns along gridline 0/1A (See Fig. 1). The Y-shaped columns allow for a larger open space in the terminal while reducing the span of the roof. Cast steel bearings were used to transfer load from V-shaped steel portion of the mixed column to lower concrete portion. Due to low redundancy and large span, the dynamic response of the roof under excitation imposes large forces and deformations on the connections. Therefore, pseudo-static test of different mixed connections between steel columns and concrete columns were performed to investigate mechanical behavior and deformation capacity.

Besides Pudong International Airport Terminal 2, mixed columns have also been utilized in the City Park in Japan (Ohnishi 2000) and the Southern Cross Station in Australia (Skene 2006). The former adopted Y-shaped tubular connections. The joints consisted of a portion of elliptic steel tube which was vertical to Y-shaped plane formed by other three tubes. In a test of this configuration, buckling was observed at the height of 1.5 times the diameter. However, the specimens were adopted above the concrete columns, the mechanical behavior of mixed connections could not be understood from the test. At the Southern Cross Station, welded Y-shaped steel columns were embedded into lower circular truncated cone tubes and concrete was pumped from the bottom of the steel tube to form mixed columns with upper steel column and lower concrete filled tube. Pseudo-Static tests of the connections between H-shaped steel columns and concrete filled steel tube pile have shown that steel columns will experience a “pull out” failure or buckling failure depending on the amount of anchorage (Takaki 2002). Additionally, the tests of mixed beams with ends of reinforced concrete or steel reinforced concrete and center of steel revealed that the stress near the joint stayed highly than that expected, and serious cracking was observed at the concrete portion of joints. Therefore, additional stirrups were suggested to enhance shear capacity and improve concrete confinement near the joints. Mixed beams fully experienced hardening process and the capacity of the specimens got increased in relation to the plastic capacity of steel portions (Sakihama 2002, Aoyama 2006).

Mixed members are different from composite members as well as hybrid system. With improved knowledge of behavior and guidance for design, mixed connections will become a viable option for an increasing number of applications. In this paper, pseudo-static tests of different mixed connections were performed. The specific objectives were to determine the weaknesses of the specimen and accordingly proposing detailed measurements; explore transfer mechanism and hysteresis characteristic of connections; investigate mechanical behavior and deformation capacity of cast steel bearing.

2. TEST PROGRAM

Based on the results from dynamic analysis of entire structure and static analysis of mixed columns (Lu 2008), the columns along the gridline 1/0A and G were selected for investigation. Six one-quarter scale specimens were designed (see Fig. 2), one representing the columns along gridline 1/0A (specimen YC2-X) and two representing the columns along gridline G (specimens YC1-X and YC1-Y). Specimens YC1-X and YC1-Y were identical except for the direction of load they were subjected to during the test. The other three specimens with same configuration were subjected to larger axial load as to examine the effect of vertical earthquake motion.

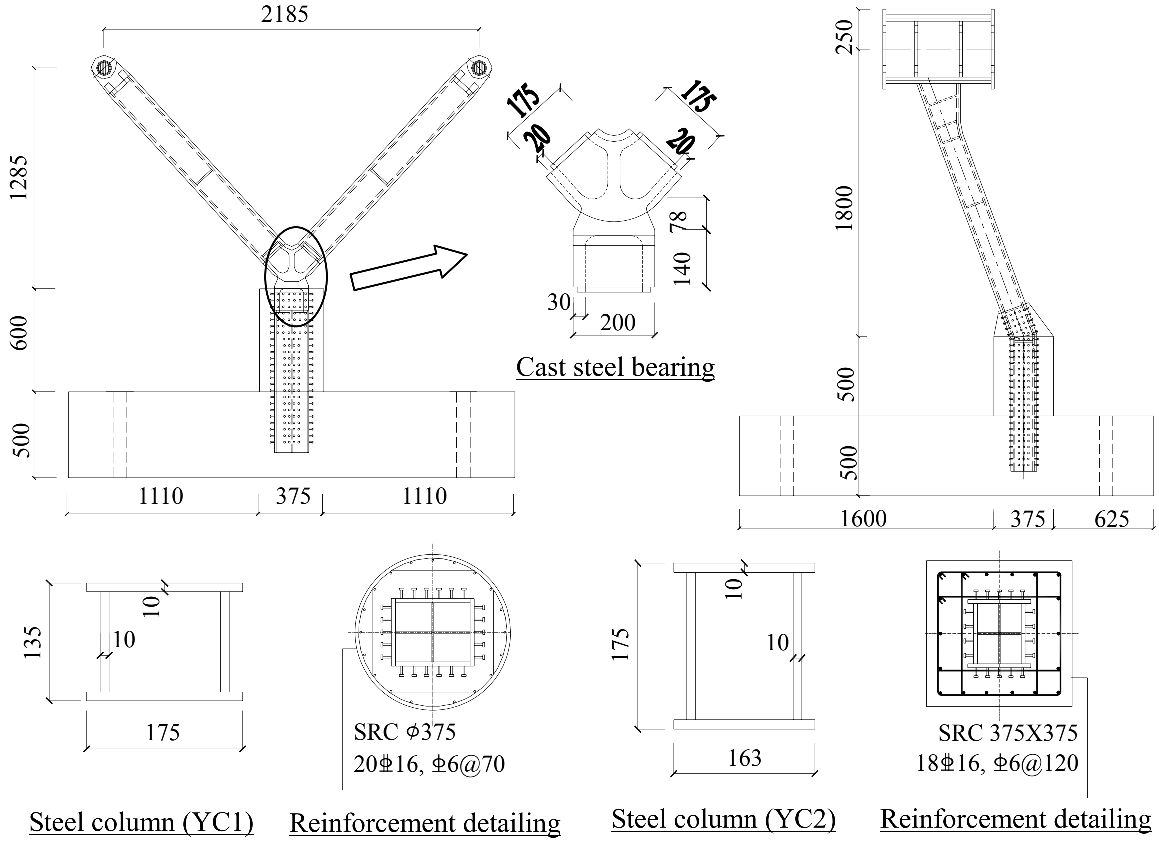

Figure 2 Detailing of specimen (mm)

2.1. Specimen Preparation

The concrete was made with Portland cement of grade 32.5, sand of fineness modulus 2.5, and aggregate with maximum size of 20mm. The mix ratio by weight was C:W:S:G=1:0.35:1:1.54 and water-reducing admixture was included at a proportion of 5% of the water quantity. Slump was designed to be 200mm ± 20 mm. After 28 days standard curing, the mean value of cubic strength was 51.4 MPa. Rolled steel parts were grade Q345B and cast steel was molded in accordance with 20Mn5 of the European Code. The results of steel properties test were showed in Fig. 3. For specimens YC1-X and YC1-Y, steel parts were fabricated separately before welding to cast steel bearings, the inclined steel columns of YC2-X were welded to lower box-shaped steel directly. Before erecting formwork, construction scaffolding and fixing welded steel on it were implemented to ensure accurate location of steel part and concrete part.

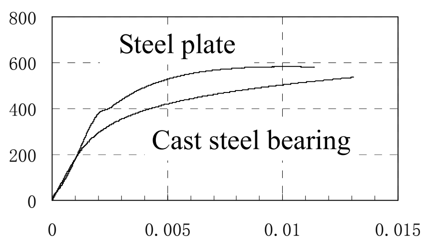

Figure 3 Property curves of steel (MPa: με)

2.2. Test setup and Measurement

The test setups are illustrated in Fig. 4. Horizontal load was imposed by an IST-100T actuator and vertical load was applied by a pair of synchronized jacks. Prior to the beginning cyclic loading for specimen YC2-X, the gravity load was applied in two stages. First, a lateral load of 36kN was applied, then 100kN vertical load was applied so as to acquire the axial load of 106kN in inclined steel column ($\tan 20^0=0.36$). A steel box beam connecting the two steel branches of specimens YC1-X and YC1-Y transferred horizontal force and transmitted the vertical load into axial load in the steel columns.

(a) YC1-X (b) YC1-Y (c) YC2-X

Figure 4 Test setup

Specimens were tested under horizontal displacement control and vertical load control. Primary measurements included: 1) LVDTs oriented in horizontal and vertical directions at the geometric center of the cast steel bearing, all pin joints for each steel column, and in the horizontal direction at the top of the concrete column and base beam 2) three inclinometers at each branch of the cast steel bearings to measure angular variation 3) strain gauges at various locations on the steel and concrete surfaces 4) evenly distributed lines on the surface of the steel near the embedment into the concrete for slip detection.

3. RESULTS AND DISCUSSION

3.1 Test Observations

3.1.1 Concrete column

The progression of damage was similar for both specimens YC1-X and YC1-Y and could be summarized below (See Fig. 4).

Due to the moment applied by the upper steel columns, flexural cracks ① at the top of concrete column initiated from the middle of the section at drift angles of 1/60 and spread to the edge of the column section at drift angles of 1/40. The minimum distance from the cast steel bearing to the crack was approximately 1.5 to 2 times the shear connector length, which might imply that they are effective to 0.5 to 1 times the connector length beyond the end of the connector. As loading increased, cracks ② starting from the corners of the cast steel bearing slanted to the edge of concrete section and converged with the initial cracks ① at drift angles of 1/30. These cracks ② could be attributed to a deficiency in shear capacity. The congregated cracks then extended down the side of concrete columns and formed crossing cracks ③ under cyclic loading. No slip was observed between the concrete and the cast steel during any stage of the loading process. This verifies that anchorage length of 3 times the depth of the steel section as well as the quantity of shear connectors specified in the Chinese Design Code provided adequate shear transfer.

The damage mode presented above showed great similarity with that of those mixed beams (Sakihama 2002). Therefore, those proposed measurements used in mixed beams could also be adopted for the mixed columns. By increasing the quantity of stirrups in the joints, the shear capacity of concrete columns can be enhanced and confinement of the outer concrete can be improved as well. The quantity of the stirrups could be determined by the moment value as well as stiffness variations near the joints. Concrete filled steel tubes could be adopted in case of large moment or steep variation of stiffness. Additionally, the longitudinal reinforcement hooks at the top of concrete section would be lengthened to improve integrity of the reinforcement cages with outer concrete.

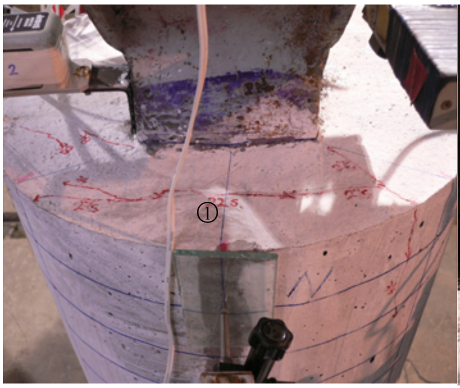

Figure 5 Cracks at the top of concrete column

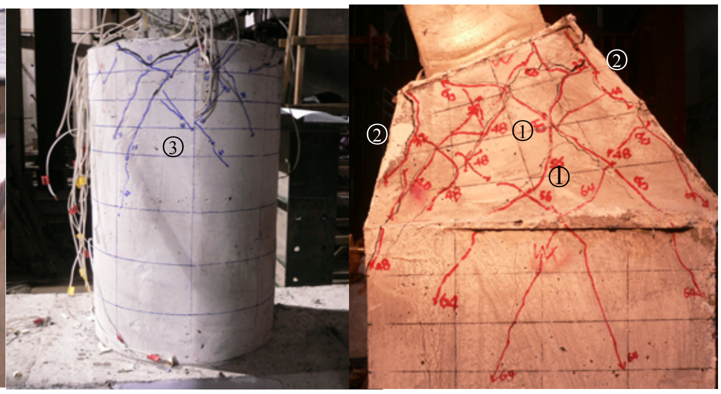

Figure 6 Cracks on the body of concrete column

For specimen YC2-X, shear connectors at flank had a striking shear effect on the concrete and thereby caused crossed cracks ① at upper segment (See Fig. 6). The diagonal cracks developed from the top of the concrete down to the turning point and proceeded to the lower segment (See Fig. 6). Flexural cracking ② was observed at each loading side, and the cracks initiated outside the reinforcement cages due to the thin thickness of the outer concrete. The cracks extended down with parallel to steel edge. Furthermore, tiny flexural cracks were found at the bottom of concrete column, and yielding of the longitudinal reinforcement was also detected at later phase of loading history. The bond between steel and concrete exhibited satisfactory behavior at all time.

3.1.2 Steel column

A t a drift angle of 1/25, the lacquer coating near certain welds started to drop off and a noticeable crack was detected in the Heat Affected Zone (HAZ), 1mm away from the weld. After some elongation for hardening, the crack extended quickly to the web (See Fig. 7) and the bearing capacity was hardly enhanced any longer. Subsequently, the growing crack led to the final rupture of steel columns. The weld of YC2-X embedded in concrete columns also experienced failure due to diminished contribution of concrete and led to the collapse of the specimen at a drift angle of 1/22.

Figure 7 Cracks in HAZ of Steel

Although the strength of the weld itself is as high as that of the base material, the material strength and the modulus of elasticity of steel in the HAZ both decrease approximate 10% (Xu et al. 2007). As a result, there exists a soft layer between weld and base material, and therefore a stress concentration is created. Furthermore, reduction of material strength leads to decreased capacity of the welded steel. The presence of shear forces also accelerates rupture of the butt weld. The above factors had a significant influence on the collapse behavior of the specimen. This type of damage behavior shows great similarity to that of steel structures in the Kobe earthquake, 1995 (Zhou 1996).

3.2 Hysteretic Characteristic

The hysteresis curves of concrete columns and steel columns are shown separately to clarify sources of deformation (See Fig. 8). It can be seen that the hysteresis curve of the concrete column remains in the elastic range before collapse of the specimen. The area enclosed by the hysteresis loops could be attributed to non-synchronization of vertical jacks in the loading process rather than inelastic behavior of the concrete column. The hysteretic curves of the steel columns show clear strain hardening branches. Strength and stiffness

reduce significantly in a degradation branch when damage occurs in the HAZ.
At later phase of loading, the hysteresis curve of the steel column of specimen YC2-X exhibits a clear deterioration. Eventually, the rupture of the steel at the weld causes the collapse of the specimen even though the concrete column also shows obvious degradation in strength and stiffness.

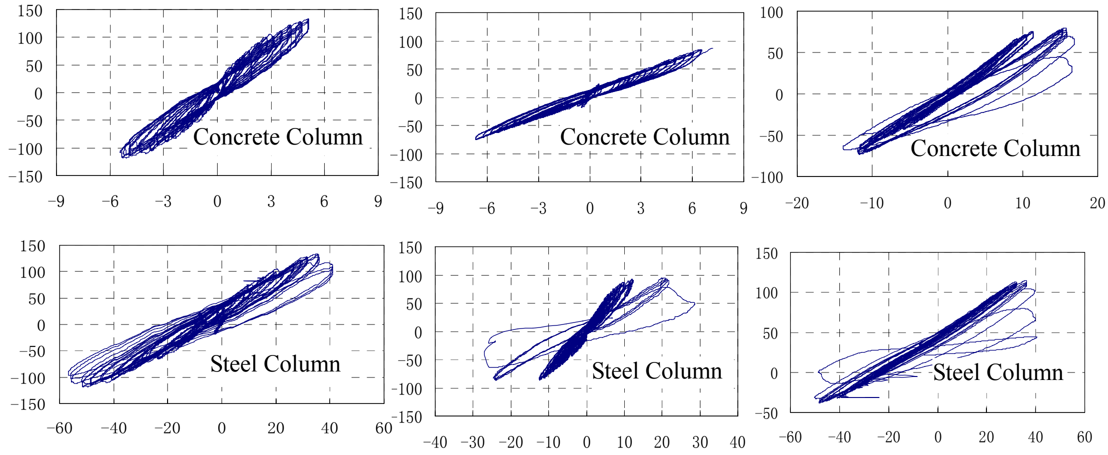

(a) YC1-X (a) YC1-Y (c) YC2-X

Fig. 8: Hysteretic Curves (kN: mm)

3.3 Force Transfer Mechanism of Cast Steel Bearing

3.3.1 Specimen YC1-X

Due to the restraint from loading beam, a vertical load of N applied to the beam becomes an axial load 1.36N in steel columns (See Fig. 9). The horizontal force applied by the actuator produces a force V and moment V*L at the pin joints of the steel columns. The horizontal force V is transferred directly to the steel columns while the moment is resisted by a couple of vertical forces of magnitude 0.19V at both pins (See Fig. 9). Rearranging axial forces and shear forces in the steel columns reveals that maximum compressive stress at the boundary with cast steel occurs at the position of V_{11} while maximum tensile stress occurs at the position of V_{12}. It is the location of maximum tensile stress where damage occurred in the test. Although yielding of the cast steel bearing is also recorded at point A (See Fig. 10b), failure of the cast steel is unlikely to occur because of its larger thickness and approximately same material strength as the steel columns. The hysteresis curve of the strain at point A is displayed in Fig 11(a).

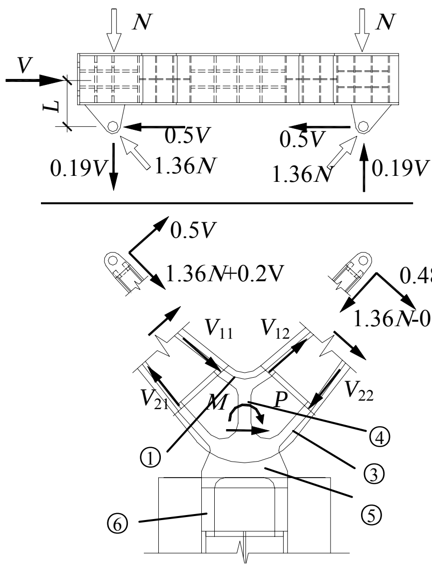

Fig. 9: Free-Body Diagram

Axial load in the steel columns distributes proportionally to the cast steel bearing in accordance with the product of modulus of elasticity and sectional area. Under the action of shear forces (See Fig. 9), the axial force V_{11} and V_{12} in the upper arc plate ① are transferred into shear force P in the internal plate ④, and also moment M_1 is induced at the bottom of internal plate. Axial force V_{21} and V_{22} transfer along lower arc plate ③. The above forces mix in solid pier body ⑤ before transferring to hollow Pier Base with definite stress state.

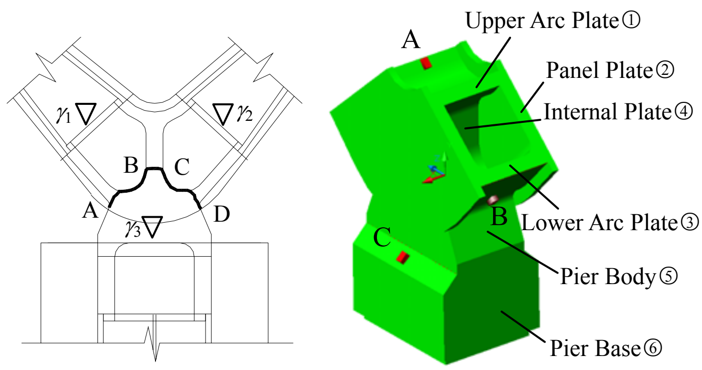

(a) Inclinometer (b) Strain

Figure 10 Monitoring points on the cast steel bearing

In the loading process, yielding was detected in the re-entrant corners of the cast steel bearing and hysteresis curve of the strain at point B (See Fig. 10b) is displayed in Fig 11(b). Although the strain inside the cast steel bearing could not be measured, a potentially critical damage section, ABCD, is located based on free body diagram, strain measurements, and findings of numerical analyses conducted previously (Zhang et al. 2007).

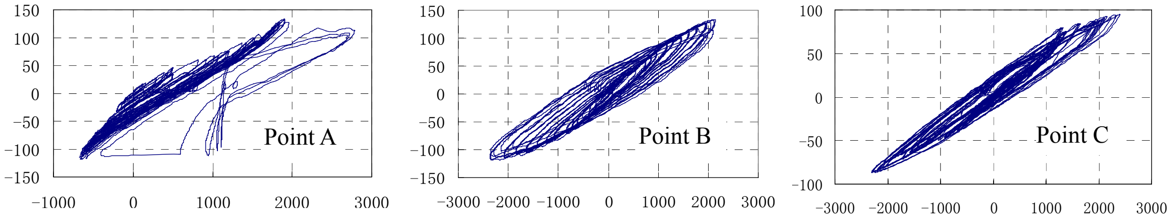

Figure 11 Load-Strain Hysteretic Curves of the Points in Figure 10b (kN: με)

Although the damage occurring in cast steel was explored in the design of the global structure, there is a finding from the test that might be beyond design. The variation in material properties of cast steel is larger than that of hot rolled steel. Striving for equal reliability in design, the capacity of cast steel bearings based on average material properties is reduced more than the capacity of hot rolled steel members. It is therefore important for the designer to estimate both the deisgn strength and the expected strength to ensure that the design objective is met, especially when designing for damage to occur in the cast steel bearing.

The presence of HAZ and over-strength of the cast material caused the rupture of the welded steel at the bottom of steel column, but it's difficult to draw the same conclusion with respect to prototype members. First, there is a distinction of moment-shear ratio at the centroid of cast steel bearing. The difference of axial forces in the asymmetry steel branches of prototype members induce a shear force in cast steel. With respect to specimens, the steel branches are symmetry and shear force could not be derived from equal axial forces at cast steel bearing. Furthermore, it is hard to identify the most adverse state of the mixed columns from a great number of loading cases. Therefore further investigations into possible weaknesses of the prototype members will be needed.

3.3.2 Specimen YC1-Y

Axial load distributes proportionally to the arc plate ①, ③ and panel plate ② in accordance with axial stiffness (Fig. 10b). Applying the shear loads, both panel plates ② resist most of the moment associated with arc plates ①, ③ and internal plates ④. The complex stress fully mixed in the solid pier body ⑤ before transmitting to the pier base ⑥. In the test, panel plates ② remained elastic and recorded maximum strains occurred at point C (See Fig. 10b and Fig. 11c) due to transformation from solid to hollow body as well as varied external dimensions. However, as the thickness of the pier base is 3 times that of the steel part below, the weakness would be transferred downwards.

3.4 Elastic Rotation Stiffness of Cast Steel Bearing

In order to investigate the mechanical behavior and deformation capacity of the cast steel bearing the rotation between the branches and elastic rotational stiffness of cast steel bearing were examined

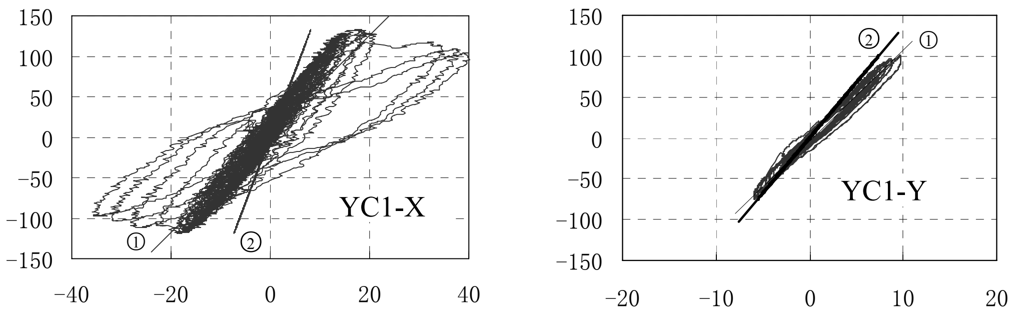

Figure 12 Rotation stiffness of bearing (kN: mm)

separately, which were used to clarify the component of the displacement at the top of steel columns. The location of three inclinometers is shown in Fig. 10a. Although the difference between the average steel column rotation and the base rotation $(r_1+ r_2)/2-r_3$ could be regarded as the rotation angle of the cast steel bearing, rotation of the steel columns is also included in r_1 and r_2. Therefore, formulation for the rotation angle of the cast steel bearing should be expressed as $r_b=(r_1+ r_2)/2-r_s-r_3$, where the rotation angle r_s was calculated in accordance with the loading state of the steel column (Chen 2001).
Elastic stiffness ① as given in Fig. 12 is derived from the hysteretic curve of rotation angle $(r_1+ r_2)/2-r_3$, and elastic stiffness of the steel column is shown as a line ②. Contrasting stiffness curves ① and ②, it is demonstrated that rotational stiffness of the cast steel bearing is 1.63 times as well as 3.88 times than that of the steel column for YC1-X and YC1-Y seperately. And therefore the rotation of the cast steel bearing is responsible for 40% and 20% of the top displacement separately unless the deformation in columns is considered.

4. CONCLUSION

Pseudo-static tests of six mixed connections representing connections in the mixed columns used in the Terminal Building 2 of Pudong International Airport were conducted. The main findings are listed below:
1) Cracking, and spalling were observed at the top of the concrete columns due to the moment applied by upper steel columns and the column stiffness variation near the joint. Suggestions for mitigating this type of damage were presented which enhance the shear capacity and improve the concrete confinement. As for large moment or steep variation in column stiffness, concrete filled steel tube could be adopted for further improving the integrity of the joint.
2) The longitudinal reinforcement hooks at the top of concrete section would be lengthened to improve integrity of the reinforcement cages with outer concrete. No slip was observed between concrete and steel in the test which verified the detailed measurement specified in the Chinese Design Code.
3）Damage occurring at the bottom of the steel column could be attributed to the modulus of elasticity and yield strength of the steel both being decreased about 10% in the Heat Affected Zone (HAZ) as well as higher expected strength of the cast steel. The damage observed shows great similarity to that of steel structures in the Kobe earthquake 1995.
4) Although the cast steel bearing remain undamaged in the test, the potential critically damage section in the bearing was identified based on free body diagrams, strain measurements, and findings of finite element analyses. Since the strength of the cast material is more inconsistent than hot rolled steel; a larger variance was used to determine the design strength. Therefore, the actual capacity of the cast steel bearing is more likely to be under-estimated, and the performance of the cast steel may not be as expected in the original design. As a result, the damage mode will possibly be switched even the yield section was designed in cast steel.
5) Transfer mechanism of the cast steel bearing was examined in accordance with analyses of free-body diagram and strain results; and elastic rotational stiffness was deduced based on the measured rotation angle, which can be used to clarify the component of the displacement at the top of steel columns.

Acknowledgements:
This work was funded by the Science and Technology Commission of Shanghai Municipality under Grant 052112011. Valuable suggestions provided by M. Denavit and M. Eatherton during the analysis and composition of the paper are gratefully acknowledged.

REFERENCES

Ohnishi, K., Komiya, N., Kikuchi, M., Sugimoto, H., Takahashi, Y. (2000). Experimental Study on Behavior of Steel Tubular Truss Y-Joints. *Summaries of Technical Papers of Annual Meeting Architectural Institute of Japan,* (C-1), 533-534.

Skene, P., and DiBlase, R. (2006). Tubular Steel Roof for Spencer Street Railway Station in Melbourne, Australia. *Weld. World,* 50, 23-30.

Takaki, J., Yamaguchi, I., Odajima, N., Kitazawa, M. (2002). Study on Structural Performance of the Joint between a Cross Sectional Column and a Cast-in-Place Concrete Pile. *Summaries of Technical Papers of Annual Meeting Architectural Institute of Japan,* (C-1), 111-114.

SAKIHAMA, H., NISHIHARA, H., SUZUKI, H. (2002). Experiment on Mixed-Structure Beam with both End of RC or SRC and Center of S. (C-1), 1055-1056.

Aoyama, N., and Minamisaka, N. (2006). Stress Transfer from Steel Member to Reinforced Concrete Member. *Summaries of Technical Papers of Annual Meeting Architectural Institute of Japan,* (C-1), 1107-1108.

Lu, X. L. (2008). *Research Report of Key Technology on Terminal Building of Pudong International Airport Phase II.* Research Institute of Structural Engineering and Disaster Reduction at Tongji University., Shanghai.

Zhang, J., Lu, X. L., Luo, W. C. (2007). Numerical Investigation of the Vertical Hybrid Columns with Cast Steel Bearings in an Airport Terminal. *Harbin Gongye Daxue Xuebao/Journal of Harbin Institute of Technology,* 39, 117-121.

Zhou, B. Z. (1996). Earthquake Damages and Lessons of Kobe Earthquake, Japan. *Earthquake Resistant Engineering,* 3(1), 39-42.

Xu, F., Zhu, M. H., Tang, Z. B., Li, Y. L. (2007). The application of ISDG method on the mechanical property measurement of the welding-line material. *Proc., Asian Pacific Conference for Fracture and Strength (APCFS'06),* Trans Tech Publications Ltd, Stafa-Zuerich, CH-8712, Switzerland, , 2724-2727.

Chen, Y. Y., Wang, W., Zhao, X. Z., Jiang, X. Y., Bai, X., Zhao, Z. Y. (2001). Experiments on Bending Rigidity and Resistance of Unstiffened Tubular Joints. *Jianzhu Jiegou Xuebao/Journal of Building Structures,* 22(6), 25-30.